

Advances in Ion Doping Strategies for $\text{LiMn}_x\text{Fe}_{1-x}\text{PO}_4$ Cathodes: Progress, Challenges, and Outlook

Ming Liang¹, Zhenwei Hu¹, Caiyi Yuan¹, Ling Chen^{1,2,3,*}, Wanxuan Yuan^{4,*}

¹School of Materials and Environment, Guangxi Minzu University, Nanning, Guangxi, China

²Guangxi Key Laboratory of Advanced Structural Materials and Carbon Neutralization, Nanning, Guangxi, China

³Guangxi Engineering Research Center for Advanced Materials and Intelligent Manufacturing, Nanning, Guangxi, China

⁴School of Intelligent Manufacturing, Guangdong Polytechnic of Water Resources and Electric Engineering, Guangzhou, Guangdong, China

Abstract: $\text{LiMn}_x\text{Fe}_{1-x}\text{PO}_4$ possesses notable advantages including high energy density, excellent safety performance, scalability for large-scale production, and low cost. Thus emerging as one of the most promising olivine-structured cathode materials. However, key technical hurdles still hinder its large-scale application, such as intrinsically low electrical conductivity and compromised cycling stability induced by the Jahn-Teller effect. Accordingly, this paper commences with an overview of the structural characteristics and underlying reaction mechanisms of lithium iron manganese phosphate $\text{LiMn}_x\text{Fe}_{1-x}\text{PO}_4$, examines the merits and limitations of Mn/Fe ratio optimization on its electrochemical performance, and provides a comprehensive review of doping modification strategies targeting distinct lattice sites of this material. Finally, the critical issues, new research directions, and perspectives on further commercialization of $\text{LiMn}_x\text{Fe}_{1-x}\text{PO}_4$ are discussed.

Keywords: Cathode Materials, Lithium Iron Manganese Phosphate, Ion Doping

1. Introduction

With the advancement of the electrochemical field, ever since Whittingham[1] first prepared lithium-ion batteries in 1976, this technology has drawn extensive research attention. Today, the development of new energy vehicles has fueled the rapid progress of lithium-ion battery materials. In recent years, olivine-structured phosphate materials for automotive power battery cathode have emerged as a prominent research focus (Figure 1). The discovery and research of olivine-structured phosphate materials LiMPO_4 ($\text{M} = \text{Mn, Co, Fe}$) can be traced back to the research report published by the Goodenough[2] team as early as 1997. Using first-principles calculations, key parameters including voltage plateau, energy density, and specific capacity of these cathodes can be derived.[3-4] Table 1 summarizes and compares these critical parameters.

Table 1 Voltage Plateau, Theoretical Specific Energy, and Theoretical Specific Capacity of LiMPO_4 ($\text{M} = \text{Mn, Co, Ni, Fe}$) Cathode.[3-4]

	Voltage Plateau	Theoretical Energy Density	Theoretical Specific Capacity
LiFePO_4	3.5 (vs. Li)/V	683.5 Wh kg ⁻¹	169.9 mAh g ⁻¹
LiMnPO_4	4.1 (vs. Li)/V	713.5 Wh kg ⁻¹	170.9 mAh g ⁻¹
LiCoPO_4	4.8 (vs. Li)/V	816.4 Wh kg ⁻¹	166.6 mAh g ⁻¹

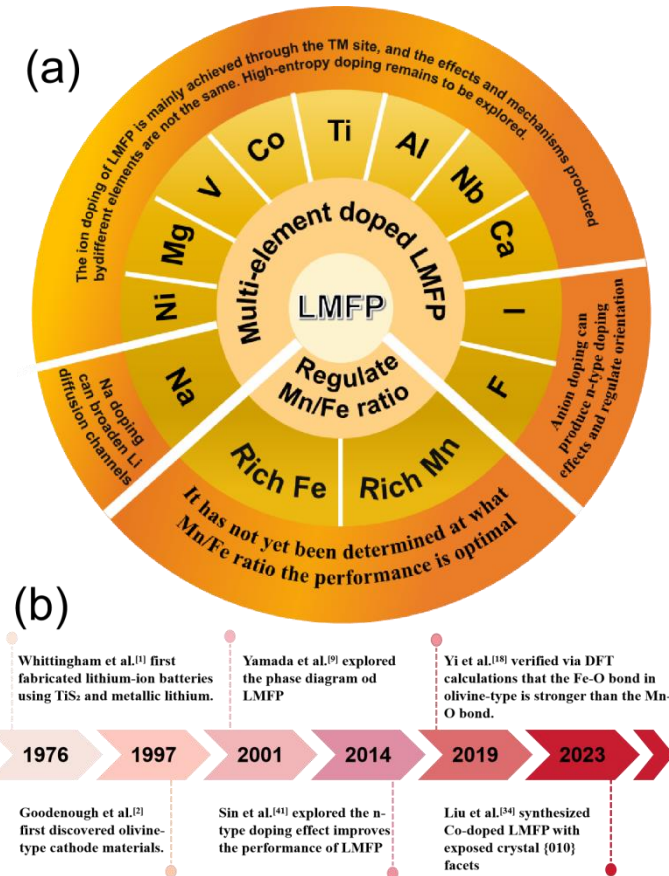


Figure 1 (a)Timeline diagram of partial typical works related to the structure and mechanism of olivine type $LiMnxFe1-xPO_4$. (b)Brief summary of Mn/Fe ratio regulation and element at distinct sites in LMFP cathodes.

2. Structural characteristics and lithium storage mechanism of $LiMnXFe1-XPO_4$

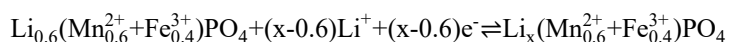
The structure of $LiMPO_4$ ($M = Mn, Co, Fe$) adopts an olivine-type crystal structure, which crystallizes in the orthorhombic system with the $Pnma$ space group. The transition metal cation M (Mn, Co, Fe) coordinates with O to form MO_6 octahedra, while P bonds with O to constitute PO_4 tetrahedra.^[5] Notably, the strong covalent P-O bonds make oxygen extraction from the crystal lattice highly unfavorable, thereby endowing olivine-structured phosphate materials with excellent stability and safety. As shown in Figure 2a, the $LiFePO_4$ (LFP) unit cell forms a well-ordered spatial structure with tetrahedral PO_4 and octahedral FeO_6 and LiO_6 distributed alternately.^[6-7] $LiCoPO_4$ suffers from high Co costs and a relatively low theoretical specific capacity, while $LiMnPO_4$ (LMP) is intrinsically an insulator with a band gap of 2eV.^[8] Among these olivine phosphates, only LFP has extensively adopted as a cathode material for new energy vehicle power batteries, owing to its excellent safety, environmental benignity, and low cost-effectiveness.

However, the low electronic conductivity, ionic conductivity, and operating voltage of LFP result in poor rate performance, hindering its ability to meet the growing electrochemical performance demands for power cathode materials. To overcome this limitation, researchers developed the $LiFe_{1-x}Mn_xPO_4$ (LMFP) cathode material, drawing on the structural similarity between LFP and LMP, and the small ionic radius difference between Fe^{2+} and Mn^{2+} —properties that allow Mn and Fe to form solid solutions in any proportion.^[9-10] As early as 2001, Yamada et al.^[11] investigated the reaction mechanisms of the LMFP system:

Two-phase reaction: ($0 \leq x \leq 0.6$, 4V, Mn^{3+}/Mn^{2+})



Single-phase reaction: ($0.6 \leq x \leq 1.0$, 3.5V, Fe^{3+}/Fe^{2+})



The development of LMFP simultaneously mitigates LFP's low voltage platform and LMP's poor electrical conductivity[12-13], exhibiting commercial potential to replace LFP. Figure 2b shows that LMFP shares a similar crystal structure with LFP and LMP, all adopting an olivine structure where MO_6 octahedra ($\text{M} = \text{Mn, Fe}$) are interconnected with PO_4 tetrahedra.[14] Lithium ions exhibit facile intercalation and deintercalation, facilitated by the polyanionic nature of this three-dimensional framework.

While LMFP exhibits relatively high structural stability, the incorporation of Mn inevitably induces the Jahn-Teller effect, triggering Mn dissolution.[15] Although Mn content correlates positively with LMFP's voltage platform, the Jahn-Teller effect of Mn^{3+} and electrostatic repulsion between Mn^{2+} and P^{5+} , cause elongation of Mn-O bonds in edge-sharing PO_4 tetrahedra. Upon delithiation, Mn^{3+} migrates toward lithium-ion diffusion channels[16], which ultimately reduces lithium intercalation capacity and severely degrades the battery's electrochemical performance.(Figure 2c)

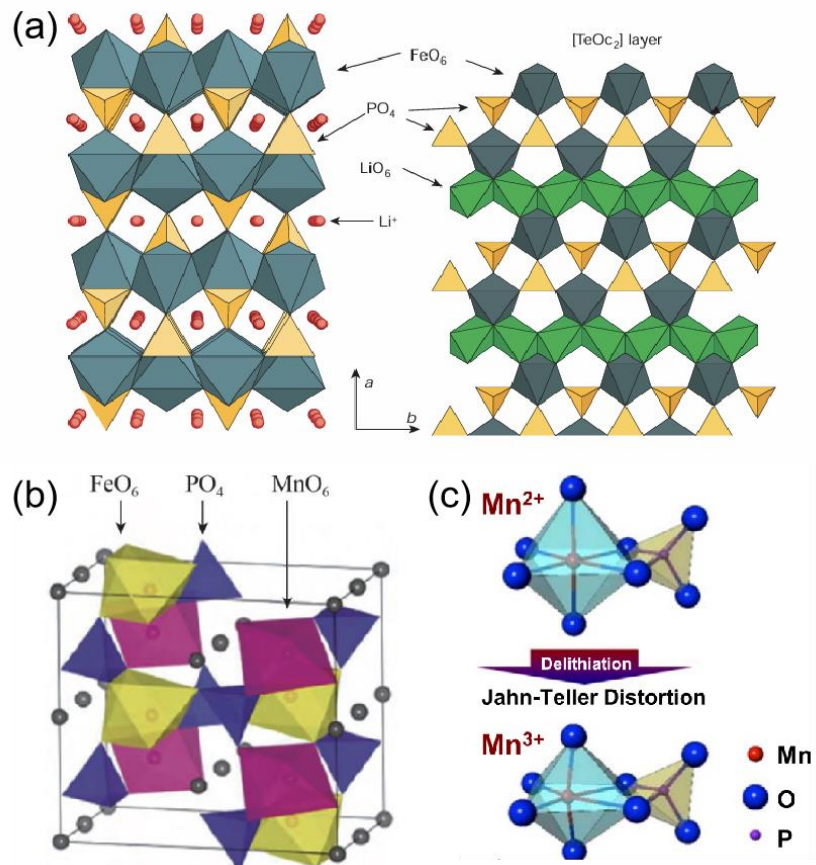


Figure 2 (a)Schematic diagram of the LFP crystal structure projected along the [001] direction.[6] (b)Schematic diagram of the $\text{LiFe1-xMnxPO}_4(0 < x < 1)$ crystal structure.[14] (c)Schematic diagram of crystal structure changes induced by the Jahn-Teller effect.[15]

3. The intrinsic relationship of the Mn/Fe ratio

The performance of LMFP exhibits a general functional dependence on the Mn/Fe ratio. In general, the voltage platform and energy density of LMFP systems tend to increase with rising manganese content. However, the Jahn-Teller effect and intrinsic low conductivity of high-Mn compositions mean that tuning the Mn/Fe ratio enables the development of materials tailored to various application scenarios.[17]

LMFP with a high Mn content may be regarded as Fe-doped LMP via impedance analysis (Figure 3a), Yi et al.[18] revealed that Fe doping significantly reduces the charge transfer resistance (Figure 3b). The lithium-ion diffusion coefficient (D_{Li^+}) was calculated using the slope of Z_{ct} vs. $\omega^{0.5}$ (Figure 3c), and it can be observed from Figure 3d that D_{Li^+} increases with the amount of Fe doping. DFT calculations show that the Fe-O bond is stronger than the Mn-O bond, and it can be inferred that the thermal stability of LMFP is superior to that of LMP (Figure 3 e,f).Xiong et al.[19]

propose that the capacity loss of LMFP is mainly attributed to the phase transition of Mn^{2+}/Mn^{3+} during the charge-discharge process, which is consistent with the Jahn-Teller effect[15]. Simultaneously, both discharge voltages attain their maxima at a manganese content of 0.8.[20]

LMFP with a high Fe content is considered Mn-doped LFP, which can improve the electrochemical rate performance and cycling performance of the material.[21] Following Mn doping, the voltage platform of LFP was enhanced. As the degree of the Mn substitution increased, the redox peaks in the high-voltage region (~4V) grew more distinct (Figure 3g). Moreover, Mn incorporation also expanded the lattice constants, facilitating lithium diffusion through the one-dimensional channels on the (010) plane (Figure 3h).[22]

Recent research suggests that LMFP with a Mn/Fe ratio of 4:6 offers broader application prospects and research value. The Mn/Fe ratio corresponding to the optimal performance remains undetermined, though it is generally accepted that this ratio does not exceed 8:2.[9] Table 2 summarizes the specific capacities and corresponding capacity retention of LMFP across varying Mn/Fe ratios, while non-stoichiometric ratios, whose mechanisms remain unclear—offer novel insights for researchers.

Table 2 Electrochemical performance of LMFP with different component ratios

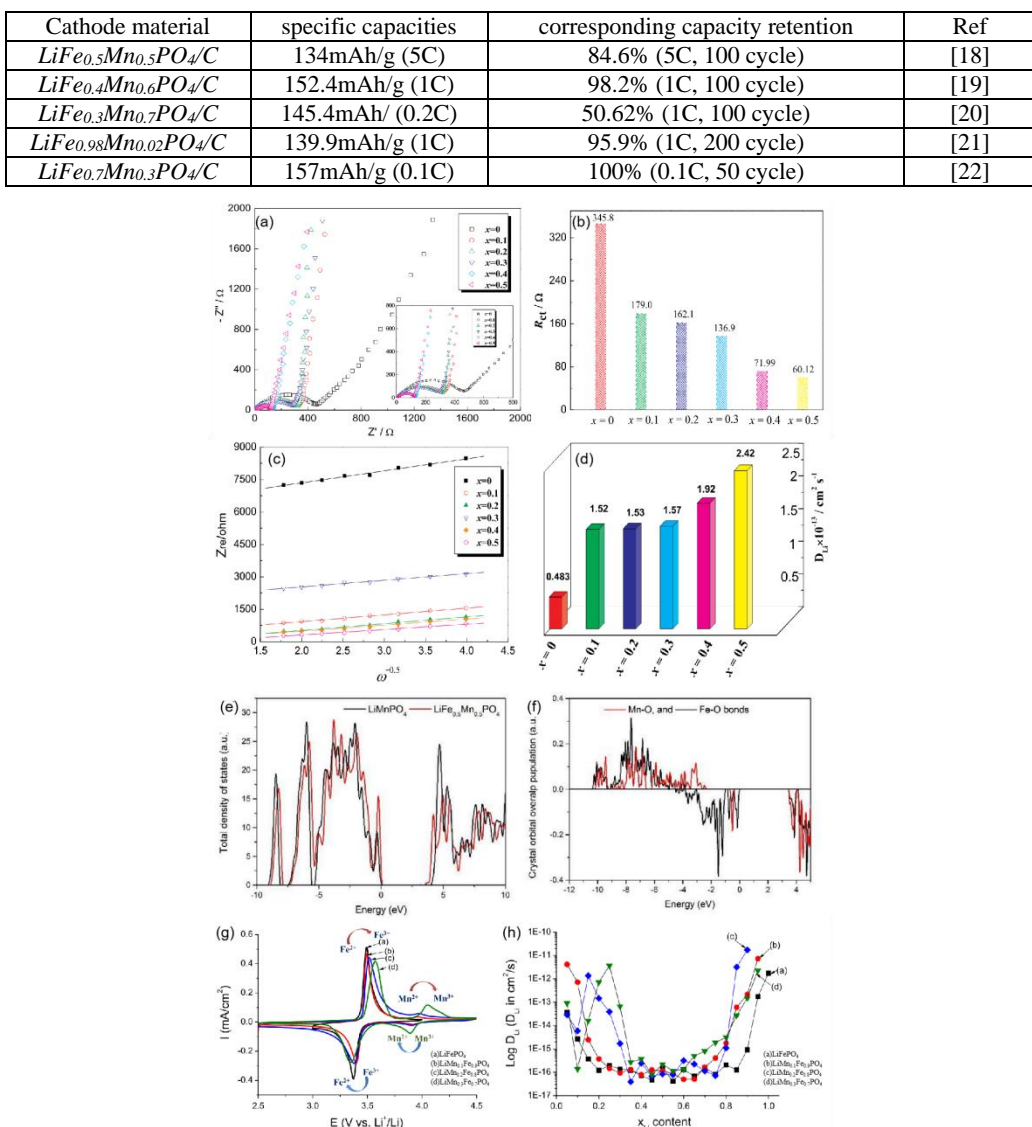


Figure 3 (a)Nyquist plots, (b)fitted values of charge transfer resistance, (c) corresponding pertinence between Z_{re} and $\omega^{-0.5}$ at the low-frequency area and, (d) calculated Li-ion diffusion coefficients for carbon-coated $LiMn1-xFexPO4(0 < x < 0.5)$, (e)Total density of states (TDOSSs) for $LiMnPO_4$ and $LiFe0.5Mn0.5PO_4$, (f) crystal orbital overlap populations (COOPs) for the M-O bonds in $LiMn0.5Fe0.5PO_4$ system.[18] (g)Cyclic voltammograms of LMFP, (h)Evolution of DLi as a function of lithium content in olivine samples.[22]

4. Other ionic doping improves LMFP performance

Ionic doping introduces lattice defects in LMFP, mitigates the Jahn-Teller effect, and accelerates lithium-ion diffusion within grains, thereby optimizing the performance of LMFP materials.[23]

Li-site doping with ions possessing larger ionic radius broadens lithium-ion diffusion channels, lower the lithium-ion activation energy barrier. Li et al.[24] performed Na^+ and Fe^{2+} co-doping on LMP and synthesized $\text{Li}_{1-x}\text{Na}_x\text{Mn}_{0.8}\text{Fe}_{0.2}\text{PO}_4/\text{C}$ nanocapsule particles via a liquid-phase method (Figure 4a). Optimal electrochemical performance was achieved at $x=0.3$, delivering a specific capacity of 125 mAh/g at 0.5C, and a capacity retention of 96.65% after 200 cycles (Figure 4b). It can be seen that the particle size of the Na-doped sample from Figure 4c and 4d reveal that Na-doping exhibits notably smaller particle sizes, indicating that Na^+ doping inhibits nanocapsule growth.

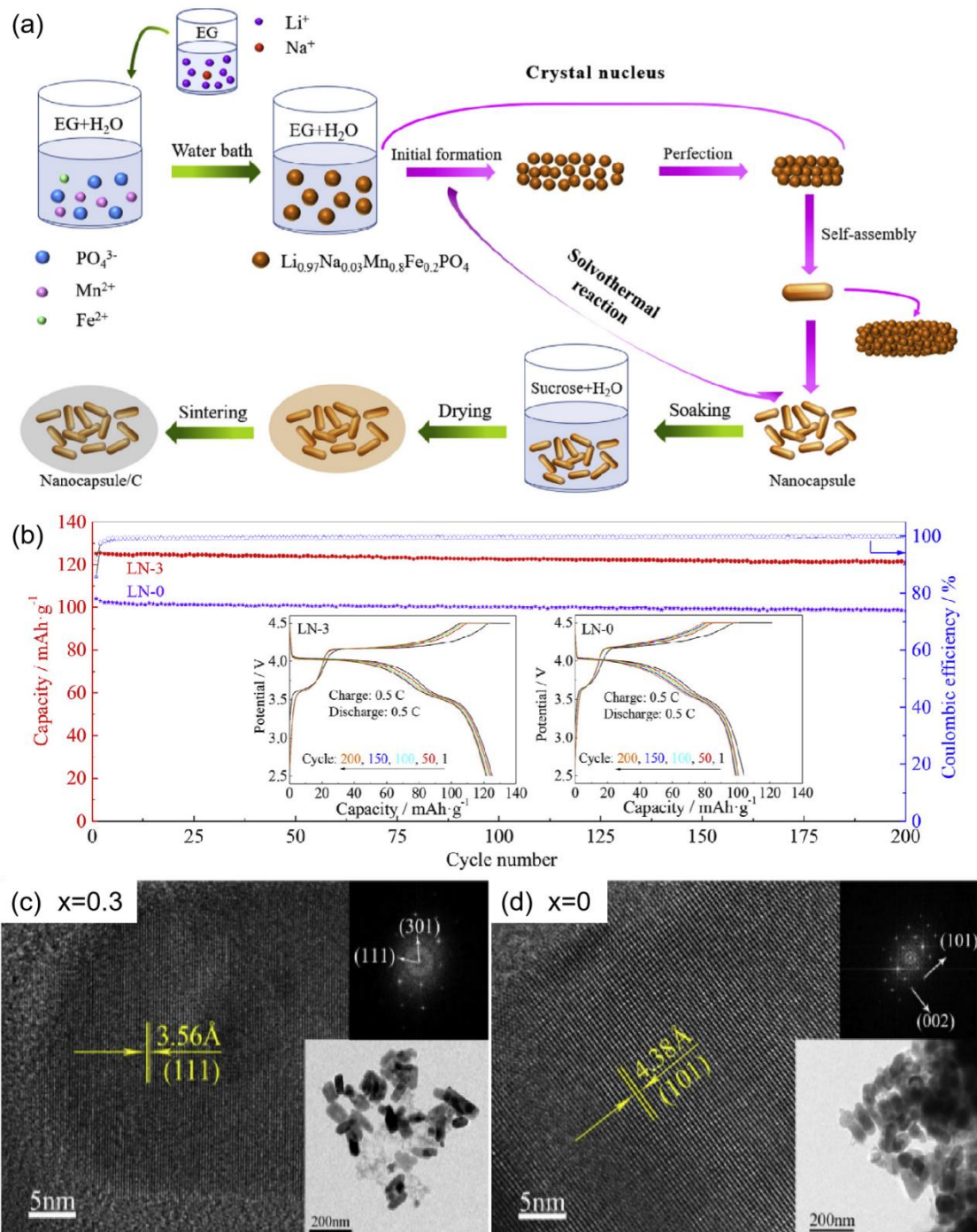


Figure 4 (a)Schematic diagram of the formation , (b)cycling performance and charge-discharge curves and (c)(d)HRTEM images of nanocapsule $\text{Li}_{1-x}\text{NaxMn}_{0.8}\text{Fe}_{0.2}\text{PO}_4/\text{C}$.[24]

The ionic doping of LMFP primarily targets the transition metal(TM) sites, and the advantages and disadvantages caused by doping this system with different metal elements differ substantially. Typical dopant elements include Ni[25-26], Mg[27-29], V[30], Co[31-32], Ti[33-34], Al[35], Nb[36], Ca[37], and others.

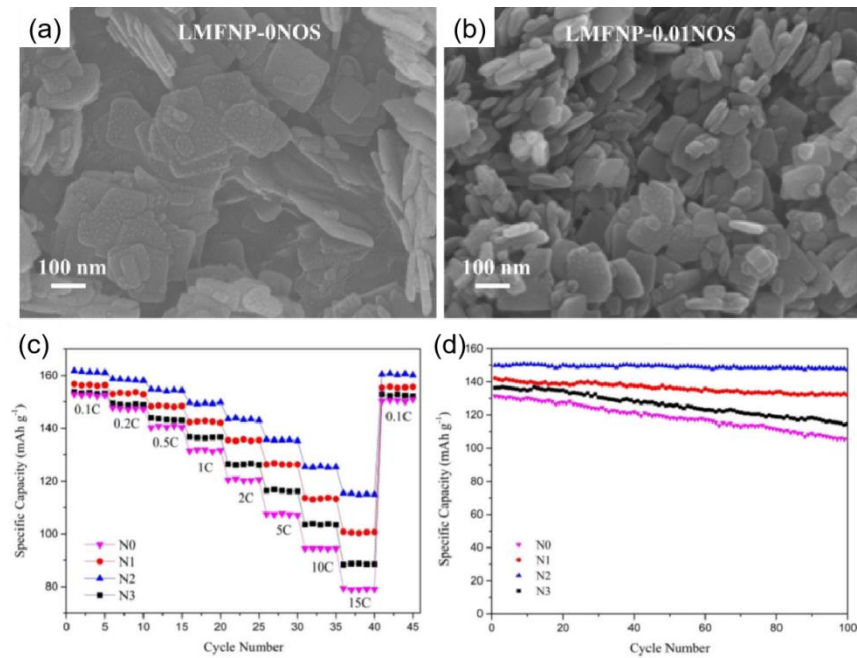


Figure 5 SEM images of $\text{LiMn}_{0.8}\text{Fe}_{0.2}\text{PO}_4$ (a) and $\text{LiMn}_{0.8}\text{Fe}_{0.19}\text{Ni}_{0.01}\text{PO}_4$ (b) samples.[25] (c)rate capability of different samples at various rates ranging from 0.1 to 15 C, (d) cycling performance of different samples at 1 C.[26]

The Ni-doped LMFP exhibits small particle sizes, uniform morphology, and a large specific surface area. Wang et al.[25] synthesized $\text{LiMn}_{0.8}\text{Fe}_{0.19}\text{Ni}_{0.01}\text{PO}_4$ with length and width both below 100 nm along the [100] direction (Figure 5a,b). Tian et al.[26] reported that optimal rate performance (Figure 5c) and cycling stability (Figure 5d) are achieved with 2mol% Ni doping. As shown in Figure 6a, Mg doping modifies the lattice parameters of the material, which expands lithium-ion transport channels and enhances the lithium-ion mobility (Figure 6b).[27] Prior research indicates that the optimal magnesium doping content for LMFP systems ranges from 1-2mol%. [28-29] Vanadium doping notably boosts the electrochemical activity of LMFP. Since (valence state +3) substitutes for Fe^{2+} (metal site valence state +2) in the lattice, it introduces vacancies that the carrier concentration in the system. And it is usually denoted by \square to represent a Fe vacancy.[30] Co doping effectively mitigates material agglomeration while improving specific capacity and cycling stability.[31] Liu et al.[32] acquired XRD patterns of {010}-oriented $\text{LiMn}_{0.7}\text{Fe}_{0.3}\text{PO}_4$ -1%Co, as shown in Figure 6c. The intensity ratios of $I_{(020)}/I_{(200)}$ for LFMP and LFMP-1%Co reaches 2.578 and 2.558, respectively (Figure 6d) indicative of an ac-facet plate-like morphology for both samples. A comparative study of the Mn dissolution at the ac and bc facets was conducted at 0 % and 100 % state of charge (SOC) (Figure 6e), Mn ions are less prone to dissolution from the ac crystal facets (Figure 6f), contributing to the material's excellent electrochemical performance. Ti doping enhances the cycling stability of LMFP.[33] Zhang et al.[34] synthesized $\text{LiMn}_{0.6}\text{Fe}_{0.38}\text{Ti}_{0.02}\text{PO}_4/\text{C}$ using TiO_2 as the Ti source, which exhibits superior low-temperature cycling performance. Aluminum(Al) doping stabilizes the LMFP structure and improves the initial capacity and capacity retention of the cathode material.[35] Niobium(Nb) doping forms Nb-O bonds that effectively alleviate the Jahn-Teller effect.[36] Meanwhile, Calcium(Ca) doping increases the lattice constants, significantly enhancing the high-rate electrochemical performance of LMFP.[37]

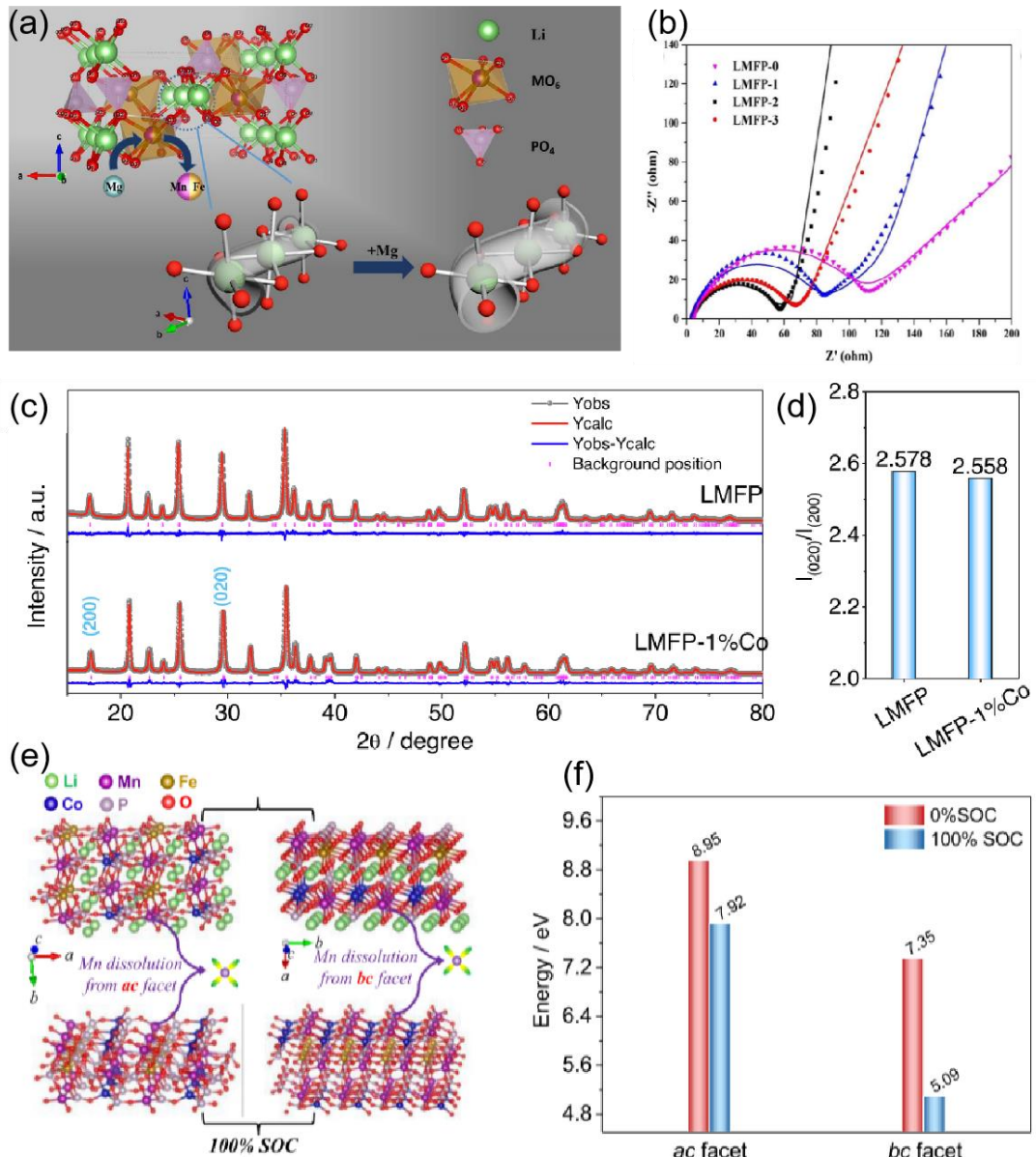


Figure 6 (a) Schematic diagram of LMFP modified by Mg-doped, (b) Nyquist plots of $\text{LiMn}_{0.6}\text{Fe}_{0.4-x}\text{Mg}_x\text{PO}_4/\text{C}$ ($x=0, 0.01, 0.02, 0.03$) samples.[28] (c) XRD patterns of LMFP and LMFP-1%Co and (d) intensity ratio of $I_{(020)}/I_{(200)}$ of XRD.(e) Graphic illustration of Mn ions dissolved from ac and bc facets at 100 % and 0 % SOC. (f) Energy needed for dissolution of Mn ions from ac and bc facets.[32]

Furthermore, anion doping also enhances the electrochemical performance of LMFP, though the underlying mechanism remains to be fully elucidated. Sin et al.[38] prepared $\text{LiFe}_{0.4}\text{Mn}_{0.6}(\text{PO}_4)_{1-x}\text{I}_x$ via a solid-state method, wherein I^- anions substitute for O^{2-} in the LMFP lattice. This material delivers a specific capacity of 102.1 mAh/g at a high rate of 3C (Figure 7a), and good cycling stability (Figure 7b). As shown in Figure 7c, F doping substitutes O sites at five distinct sites within the PO_4^{3-} tetrahedra, and the doping leads to an n-type doping effect, which in turn enhances the electrochemical performance.[39] F⁻ incorporation modulates the crystal orientation of LMFP and boosts lithium-ion diffusion kinetics.[40]

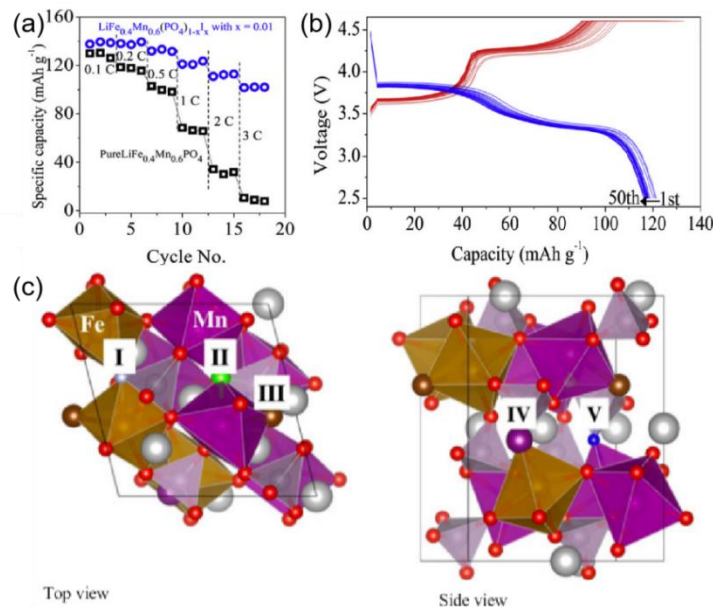


Figure 7 (a)rate performance and (b)cycle performances (at a rate of 1C between 2.5 and 4.6 V) of $\text{LiFe}_{0.4}\text{Mn}_{0.6}(\text{PO}_4)_{0.99}\text{I}_{0.01}$.[38] (c)The F-doping sites are defined by the neighboring ions sharing the substituted.[39]

With the commercialization of LMFP, tailoring doping elements to specific application scenarios can allow LMFP cathode materials to fulfill diverse requirements. The electrochemical performance and underlying mechanisms of LMFP modified via dual-element co-doping and multi-element high-entropy doping remain inadequately explored. In summary, ionic doping offers additional avenues for the modification of LMFP. Table 3 summarizes the impacts of various dopant elements on the specific capacity of LMFP.

Table 3 The effects of doping different elements on the specific capacity of LMFP.

Dopant	Cathode Material	Specific Capacity	Ref
Na	$\text{Li}_{0.97}\text{Na}_{0.03}\text{Mn}_{0.8}\text{Fe}_{0.2}\text{PO}_4/\text{C}$	141.7 mAh/g (0.05C)	[24]
Ni	$\text{LiMn}_{0.8}\text{Fe}_{0.19}\text{Ni}_{0.01}\text{PO}_4$	143 mAh/g (0.5C)	[25]
	$\text{LiMn}_{0.6}\text{Fe}_{0.38}\text{Ni}_{0.02}\text{PO}_4/\text{C}$	147.3 mAh/g (1C)	[26]
Mg	$\text{LiMn}_{0.8}\text{Fe}_{0.19}\text{Mg}_{0.01}\text{PO}_4$	122 mAh/g (1C)	[27]
	$\text{LiMn}_{0.6}\text{Fe}_{0.39}\text{Mg}_{0.01}\text{PO}_4/\text{C}$	159.6 mAh/g (2C)	[28]
	$\text{LiMn}_{0.48}\text{Fe}_{0.5}\text{Mg}_{0.02}\text{PO}_4$	160.7 mAh/g (1C)	[29]
V	$\text{LiMn}_{0.8}\text{Fe}_{0.2-0.045}\text{V}_{0.03}\square_{0.015}\text{PO}_4$	155 mAh/g (0.1C)	[30]
Co	$\text{LiFe}_{0.4}\text{Mn}_{0.4}\text{Co}_{0.2}\text{PO}_4/\text{C}$	163.3 mAh/g (1C)	[31]
	$\text{LiMn}_{0.7}\text{Fe}_{0.3}\text{PO}_4\text{-}1\%\text{Co}$	150 mAh/g (5C)	[32]
Ti	$\text{Li}(\text{Mn}_{0.85}\text{Fe}_{0.15})_{0.92}\text{Ti}_{0.08}\text{PO}_4/\text{C}$	144.4 mAh/g (1C)	[33]
	$\text{LiMn}_{0.6}\text{Fe}_{0.38}\text{Ti}_{0.02}\text{PO}_4/\text{C}$	157.8 mAh/g (0.2C)	[34]
Al	$\text{LiMn}_{0.6}\text{Fe}_{0.4}\text{PO}_4/\text{C}/\text{Al}$	168.4 mAh/g (0.1C)	[35]
Nb	$\text{LiMn}_{0.5}\text{Fe}_{0.5}\text{PO}_4/\text{C}/1\%\text{Nb}$	152 mAh/g (0.1C)	[36]
Ca	$\text{LiFe}_{0.497}\text{Mn}_{0.5}\text{Ca}_{0.03}\text{PO}_4/\text{C}$	162.6 mAh/g (0.1C)	[37]
I	$\text{LiFe}_{0.4}\text{Mn}_{0.6}(\text{PO}_4)_{0.985}\text{I}_{0.015}$	141.5 mAh/g (0.1C)	[38]
F	$\text{LiFe}_{0.4}\text{Mn}_{0.6}\text{PO}_{3.97}\text{F}_{0.03}$	153 mAh/g (0.1C)	[39]
	$\text{LiMn}_{0.5}\text{Fe}_{0.5}\text{PO}_4/\text{C}-1\%\text{F}$	106 mAh/g (5C)	[40]

5. Conclusion and outlook

$\text{LiMn}_x\text{Fe}_{1-x}\text{PO}_4$ emerges as a promising olivine-structured cathode material for lithium-ion batteries, integrating key merits including high energy density, good safety, low cost, and scalability for large-scale production. While LMFP incorporates the high conductivity of LFP and the high energy density of LMP, its widespread application is constrained by intrinsic limitations such as low electronic and ionic conductivity, compromised cycling stability arising from the Jahn-Teller effect of Mn^{3+} , and an unclear optimal Mn/Fe ratio. Over the past decades, substantial advances have been achieved in

understanding LMFP's structural features, lithium storage mechanisms, and modification strategies of LMFP, particularly in optimizing the Mn/Fe ratio and ionic doping modifications. These efforts have laid a robust foundation for the material's practical implementation.

Future research on LMFP may center on three key directions. Firstly, lattice distortion and Mn dissolution induced by the Jahn-Teller effect remain core bottlenecks restricting cycling stability. Subsequent studies should prioritize optimizing the crystal structure and mitigating the Jahn-Teller effect via ionic doping, with further efforts to elucidate the microscopic mechanisms underlying Mn³⁺ migration and crystal evolution changes during charge-discharge cycles under different ion dopings conditions. Second LMFP's intrinsic one-dimensional lithium-ion diffusion channels give rise to sluggish ion transport kinetics. Future investigations may integrate first-principles calculations, machine learning and advanced characterization techniques to explore strategies for widening lithium-ion diffusion channels and lowering activation energy barriers. Third, LMFP research should not be confined to laboratory-scale investigations. Future work should focus on identifying the appropriate optimal Mn/Fe ratio under practical operating conditions such as power batteries and large-scale energy storage to match real-world applications demands. There is also a need to develop eco-friendly synthesis routes with large-scale industrial production, thereby advancing the practical application of energy storage technologies.

Acknowledgments

This project was supported by Guangxi Higher Education Undergraduate Teaching Reform Project (2022JGA171), Scientific Research Project of Guangxi Minzu University (2020KJYB001), 2023 Autonomous Region-Level College Students' Innovation and Entrepreneurship Training Program (S202310608201), the Horizontal Project of Shenzhen Dehanda Vacuum Coating Co., Ltd. (RH2500001682) and Teaching Reform Project of Guangxi Minzu University (2021XJGY38).

References

- [1] Whittingham M S. Electrical energy storage and intercalation chemistry. *Science*, 1976, 192(4244): 1126-1127.
- [2] Padhi A K, Nanjundaswamy K S, Goodenough J B. Phospho-olivines as positive-electrode materials for rechargeable lithium batteries. *Journal of the electrochemical society*, 1997, 144(4): 1188.
- [3] Li G, Azuma H, Tohda M. LiMnPO₄ as the cathode for lithium batteries. *Electrochemical and Solid-State Letters*, 2002, 5(6): A135.
- [4] Okada S, Sawa S, Egashira M, et al. Cathode properties of phospho-olivine LiMPO₄ for lithium secondary batteries. *Journal of Power Sources*, 2001, 97: 430-432.
- [5] Shi Zhicong, Yang Yong. Progress in Polyanion-Type Cathode Materials for Lithium Ion Batteries. *Progress in Chemistry*, 2005(04):604-613.
- [6] Tarascon J M, Armand M. Issues and challenges facing rechargeable lithium batteries. *nature*, 2001, 414(6861): 359-367.
- [7] Hu J, Huang W, Yang L, et al. Structure and performance of the LiFePO₄ cathode material: from the bulk to the surface. *Nanoscale*, 2020, 12(28): 15036-15044.
- [8] Yamada A, Hosoya M, Chung S C, et al. Olivine-type cathodes: Achievements and problems. *Journal of Power Sources*, 2003, 119: 232-238.
- [9] Yamada A, Kudo Y, Liu K Y. Phase Diagram of Li_x(Mn_yFe_{1-y})PO₄(0≤x, y≤1). *Journal of the Electrochemical Society*, 2001, 148(10): A1153.
- [10] Li G, Azuma H, Tohda M. Optimized LiMn_yFe_{1-y}PO₄ as the Cathode for Lithium Batteries. *Journal of the Electrochemical Society*, 2002, 149(6): A743.
- [11] Yamada A, Kudo Y, Liu K Y. Reaction mechanism of the olivine-type Li_x(Mn_{0.6}Fe_{0.4})PO₄(0≤x≤1). *Journal of the Electrochemical Society*, 2001, 148(7): A747.
- [12] Osorio-Guillén J M, Holm B, Ahuja R, et al. A theoretical study of olivine LiMPO₄ cathodes. *Solid State Ionics*, 2004, 167(3-4): 221-227.
- [13] Yang H, Fu C, Sun Y, et al. Fe-doped LiMnPO₄@C nanofibers with high Li-ion diffusion coefficient. *Carbon*, 2020, 158: 102-109.
- [14] Zhan Haobo, Liu Shiqi, Wang Qing, et al. Research Progress on Lithium-Ion Battery Lithium Manganese Iron Phosphate Cathode Materials. *Chinese Journal of Rare Metals*, 2023, 47(12): 1669-1688. (in Chinese)

[15] Wi S, Park J, Lee S, et al. Synchrotron-based x-ray absorption spectroscopy for the electronic structure of $\text{Li}_{x}\text{Mn}_{0.8}\text{Fe}_{0.2}\text{PO}_4$ mesocrystal in Li^+ batteries. *Nano Energy*, 2017, 31: 495-503.

[16] Jiang Xin. Failure Analysis of Pouch Cells using Lithium Manganese Iron Phosphate as Cathode Material. *Chemical Industry Times*, 2020, 34(10): 5-9+44. (in Chinese)

[17] Zhao Qiuping, Li Xiangfei, Li Chunlei, Li Shiyu, Xue Yuzhou. Research development of $\text{LiMn}_{1-x}\text{Fe}_x\text{PO}_4/\text{C}$ anode material preparation and performance. *New Chemical Materials*, 2016, 44(09): 53-55.

[18] Yi T F, Peng P P, Fang Z, et al. Carbon-coated $\text{LiMn}_{1-x}\text{Fe}_x\text{PO}_4$ ($0 \leq x \leq 0.5$) nanocomposites as high-performance cathode materials for Li-ion battery. *Composites Part B: Engineering*, 2019, 175: 107067.

[19] Xiong Y, Wei Y, Rong W, et al. Preparation and electrochemical properties of carbon-coated $\text{LiMn}_{0.6}\text{Fe}_{0.4}\text{PO}_4$ cathode material for lithium-ion batteries. *ECS Journal of Solid State Science and Technology*, 2022, 11(11): 113001.

[20] Shangmin Gong, Xue Bai, Rui Liu, Hongquan Liu, Yi-jie Gu. Study on discharge voltage and discharge capacity of $\text{LiFe}_{1-x}\text{Mn}_x\text{PO}_4$ with high Mn content. *Journal of Materials Science: Materials in Electronics*, 2020, 31(10): 7742-7752.

[21] Chen W, Song F, Yang Y, et al. Mn-doped $\text{LiFePO}_4@\text{C}$ as a high-performance cathode material for lithium-ion batteries. *Particuology*, 2024, 90: 418-428.

[22] Trinh D V, Nguyen M T T, Dang H T M, et al. Hydrothermally synthesized nanostructured $\text{LiMn}_x\text{Fe}_{1-x}\text{PO}_4$ ($x=0-0.3$) cathode materials with enhanced properties for lithium-ion batteries. *Scientific Reports*, 2021, 11(1): 12280.

[23] Xu E, Sun X, Lyu W, et al. Optimizing the Electrochemical Performance of Olivine $\text{LiMn}_x\text{Fe}_{1-x}\text{PO}_4$ Cathode Materials: Ongoing Progresses and Challenges. *Industrial & Engineering Chemistry Research*, 2024.

[24] Li R, Fan C, Zhang W, et al. Structure and performance of Na^+ and Fe^{2+} co-doped $\text{Li}_{1-x}\text{Na}_x\text{Mn}_{0.8}\text{Fe}_{0.2}\text{PO}_4/\text{C}$ nanocapsule synthesized by a simple solvothermal method for lithium ion batteries. *Ceramics International*, 2019, 45(8): 10501-10510.

[25] Wang Y, Yang H, Wu C Y, et al. Facile and controllable one-pot synthesis of nickel-doped $\text{LiMn}_{0.8}\text{Fe}_{0.2}\text{PO}_4$ nanosheets as high performance cathode materials for lithium-ion batteries. *Journal of Materials Chemistry A*, 2017, 5(35): 18674-18683.

[26] Tian S Y, Zhang K C, Cao J R, et al. Spherical Ni-doped $\text{LiMn}_{0.6}\text{Fe}_{0.4}\text{PO}_4/\text{C}$ composites with high-rate performance. *Ionics*, 2021, 27(7): 2877-2887.

[27] Chu X, Li L, Chen W, et al. Hydrothermal synthesis and electrochemical performance of multicomponent $\text{LiMn}_{0.8}\text{Fe}_{0.19}\text{Mg}_{0.01}\text{PO}_4$. *Ionics*, 2021, 27(7): 2927-2935.

[28] Zhang K, Cao J, Tian S, et al. The prepared and electrochemical property of Mg-doped $\text{LiMn}_{0.6}\text{Fe}_{0.4}\text{PO}_4/\text{C}$ as cathode materials for lithium-ion batteries. *Ionics*, 2021, 27(11): 4629-4637.

[29] Zou B K, Shao Y, Qiang Z Y, et al. LiMPO₄ and derived NaMPO₄ ($M = \text{Mn, Fe, Mg}$) with excellent electrochemical properties for lithium/sodium ion batteries. *Journal of Power Sources*, 2016, 336: 231-239.

[30] Wu T, Liu J, Sun L, et al. V-insertion in $\text{Li}(\text{Fe, Mn})\text{FePO}_4$. *Journal of Power Sources*, 2018, 383: 133-143.

[31] Huang Z G, Li J T, Wang K, et al. Synthesis of $\text{LiFe}_{0.4}\text{Mn}_{0.4}\text{Co}_{0.2}\text{PO}_4/\text{C}$ cathode material of lithium ion battery with enhanced electrochemical performance. *Journal of Alloys and Compounds*, 2019, 782: 413-420.

[32] Liu S, Zheng J, Zhang B, et al. Engineering manganese-rich phospho-olivine cathode materials with exposed crystal {010} facets for practical Li-ion batteries. *Chemical Engineering Journal*, 2023, 454: 139986.

[33] Huang Q Y, Wu Z, Su J, et al. Synthesis and electrochemical performance of Ti-Fe co-doped LiMnPO_4/C as cathode material for lithium-ion batteries. *Ceramics International*, 2016, 42(9): 11348-11354.

[34] Zhang Kaicheng. Study on Synthesis and modification of Lithium Manganese Iron Phosphate Cathode Materials, Master's Thesis, Hebei University of Technology, Hebei. 2022

[35] Yang Zhou. Preparation and modification of lithium manganese iron phosphate cathode material $\text{LiMn}_{0.6}\text{Fe}_{0.4}\text{PO}_4/\text{C}$. Master's Thesis, Tianjin University of Technology, Tianjin. 2024

[36] Jin H, Zhang J, Qin L, et al. Dual modification of olivine $\text{LiFe}_{0.5}\text{Mn}_{0.5}\text{PO}_4$ cathodes with accelerated kinetics for high-rate lithium-ion batteries. *Industrial & Engineering Chemistry Research*, 2023, 62(2): 1029-1034.

[37] Liu W, Liu X, Hao R, et al. Contribution of calcium ion doping to the rate property for $\text{LiFe}_{0.5}\text{Mn}_{0.5}\text{PO}_4/\text{C}$. *Journal of Electroanalytical Chemistry*, 2023, 929: 117117.

[38] Sin B C, Singh L, An J E, et al. Enhanced electrochemical performance and manganese redox

activity of $LiFe_{0.4}Mn_{0.6}PO_4$ by iodine anion substitution as cathode material for Li-ion battery. Journal of Power Sources, 2016, 313: 112-119.

[39] *Sin B C, Lee S U, Jin B S, et al. Experimental and theoretical investigation of fluorine substituted $LiFe_{0.4}Mn_{0.6}PO_4$ as cathode material for lithium rechargeable batteries. Solid State Ionics, 2014, 260: 2-7.*

[40] *YU Songmin, JIN Hongbo, YANG Minghu, et al. Synthesis and modification of F-doped olivine $LiFe_{0.5}Mn_{0.5}PO_4$ cathode materials for Li-ion batteries. Chemical Industry and Engineering Progress, 2024, 43(01):302-309.*